Proceedings of the Research Institute of Atmospherics,
Nagoya University, Vol. 36, No. 2 (1989)

IONOSPHERIC INCOHERENT SCATTER MEASUREMENTS WITH THE MU RADAR: OBSERVATIONS DURING THE LARGE MAGNETIC STORM OF 6–8 FEBRUARY 1986

W.L. Oliver[1,2], S. Fukao[1], T. Sato[1], T. Tsuda[1], S. Kato[1], I. Kimura[3]
A. Ito[3], T. Saryou[4], T. Araki[4]

[1] Radio Atmospheric Science Center, Kyoto University, Uji, Kyoto 611, Japan
[2] Department of Electrical, Computer, and Systems Engineering, Boston University, Boston, Massachusetts 02215, USA
[3] Department of Electrical Engineering, Kyoto University, Kyoto 606, Japan
[4] Data Analysis Center for Geomagnetism and Spacemagnetism, Kyoto University, Kyoto 606, Japan

Abstract

The MU (Middle and Upper atmosphere) radar of Japan is a 46.5-MHz, pulse-modulated, monostatic, Doppler radar with an active phased-array antenna which consists of 475 crossed Yagis. This system has been used primarily, since its initial observations with a partial system in 1983, to observe the coherent backscatter from irregularities in the troposphere, stratosphere, and mesosphere (MST radar). However, this system was also designed to be able to observe the weak incoherent scatter (IS) from the free electrons of the ionosphere. We report here the MU radar IS observations made during the strong geomagnetic storm of 6–8 February 1986. During this period the MU radar observed the echo power (an approximate measure of electron density) simultaneously in four antenna beam positions. Coincident with the rise in the K_p index from 3+ to 6− near 18 LT (9 UT) on 7 February the MU radar detected the beginning of several hours of wave activity having a period of 100 minutes. By correlating the density observations in the different beams and at different altitudes, we were able to compute the phase speed (410 m/s), direction of travel (19° west of south), and horizontal (2500 km) and vertical (290–490 km) wavelength of the wave. The F-layer peak density and height oscillated during this nighttime period, and we consider several mechanisms that might cause these effects. We find that the density oscillation was too large to be caused solely by wave dynamics. We suggest that an in-flux of ionization from the plasmasphere, and a wave-induced modulation of the assimilation of this plasma flux into the ambient density, may have been the cause of the observed density increases. During the following morning (8 February) the F-layer density was observed to

become increasingly large while the layer peak height dropped, and we also consider the cause for this effect.

1. Introduction

The Japanese MU (Middle and Upper atmosphere) radar is the newest of the large atmospheric radars capable of detecting the incoherent backscatter (IS) from the free electrons in the ionosphere. This radar system has been recently described by Fukao et al. (1985a,b). The radar began operation with a partial system in 1983 and was completed in 1984. Initial observations from the middle and lower atmosphere have been published by Kato et al. (1984, 1986), among others. Ionospheric incoherent scatter observations commenced in December 1985. Sato et al. (1989) have discussed the sensitivity of the MU radar for IS detection and presented examples of typical electron density, electron and ion temperature, and ion drift velocity measurements made with this system. Oliver et al. (1988) have discussed initial observations of F-region electrodynamics with the MU radar. In this paper, we report the MU radar observations collected during the large geomagnetic storm of 6–8 February 1986. In particular, we present the electron density observations

Table 1. Basic Parameters of the MU Radar

Parameter	Value	
Location	Shigaraki, Shiga, Japan (34.85°N, 136.10°E)	
Geomagnetic parameters (300 km altitude)	Field strength:	0.0402 mT
	Declination:	5.7°W
	Dip angle:	48.3°
	Dip latitude:	29.3°
Operational frequency	46.5 MHz	
Antenna	Active phased array, 103-meter diameter circular array of 475 crossed Yagis	
aperture	8330 m^2	
steerability	0° – 30° off zenith, 5° azimuth steps, steering possible each IPP	
partitioning	25 groups of 19 elements each, each separately driveable	
Transmitter	475 solid-state amplifiers (one for each antenna element), 2.4 kW peak (120 W average) power each	
peak power	1 MW maximum	
average power	50 kW maximum	
pulse length	1 – 512μs	
IPP	400μs – 65 ms	
pulse compression	Up to 32-bit binary phase coding, Barker and complementary codes in use	

made above the radar and correlate the time series observed in different pointing directions to determine the properties of the large-scale TID observed passing over the radar for a duration of several hours.

2. The MU Radar

Fukao et al. (1985a,b) have discussed the MU radar system and Sato et al. (1989) have discussed its sensitivity for IS measurements in detail. Here we give a brief summary of the characteristics of the radar of particular pertinence to the electron density studies of interest in this paper. Table 1 lists several of the basic characteristics of the MU radar.

The MU radar is a monostatic radar with an active phased-array system. The antenna is a circular array of 475 crossed Yagi elements having a total diameter of 103 meters. Each antenna element is connected to a separate low-power transmit-receive module which can be driven coherently with low level pulses. Because all of the phase shifting and signal division/recombination is carried out at low power, the antenna may be phased to observe in different directions on a pulse-by-pulse basis, or up to 2500 times per second. This is a major advantage of the MU radar: its effective capability to observe in multiple directions simultaneously.

The major detriment for IS operation with the MU radar is the high system noise temperature of about 10000 K. This is unavoidable galactic background noise encountered at the MU radar operating frequency. Its effect is to degrade the signal-to-noise ratio achievable and to render the MU radar considerably less sensitive than most of the other routinely operating IS radars in the world. Nevertheless, Sato et al. (1989) have calculated that for a long-pulse ($500-\mu s$) power measurement signal-to-noise values in excess of unity are achievable with the MU radar, such that it can perform essentially as well as any of the other IS radars for such a measurement. On the other hand, for the very important spectral measurement, with its requirement for the transmission of a waveform of shorter pulses, it was found that the MU radar signal-to-noise ratio often drops in practice to only a few percent, such that long integration times are required to achieve acceptable statistical accuracy.

The MU radar experiment conducted during the 6–8 February 1986 period was a backscattered power measurement, from which the electron density can be estimated. A 7-bit Barker-coded pulse with a $64-\mu s$ sub-pulse width was used, providing a 9.6-km range resolution. The full power and duty-cycle of the transmitter were used for this experiment. The measurements were made throughout the E and F regions. The E-region signals are often contaminated by echoes from meteors (Sato et al., 1989). The F-region signal often becomes unusable beyond 600 km altitude owing to weak signal strength. This experiment alternated four beam positions, geographic north, east, south, and west, all at 20° zenith angle. The received power P_r is related to the electron density N_e as

$$P_r = \frac{CN_e}{R^2(1+T_r)} \tag{1}$$

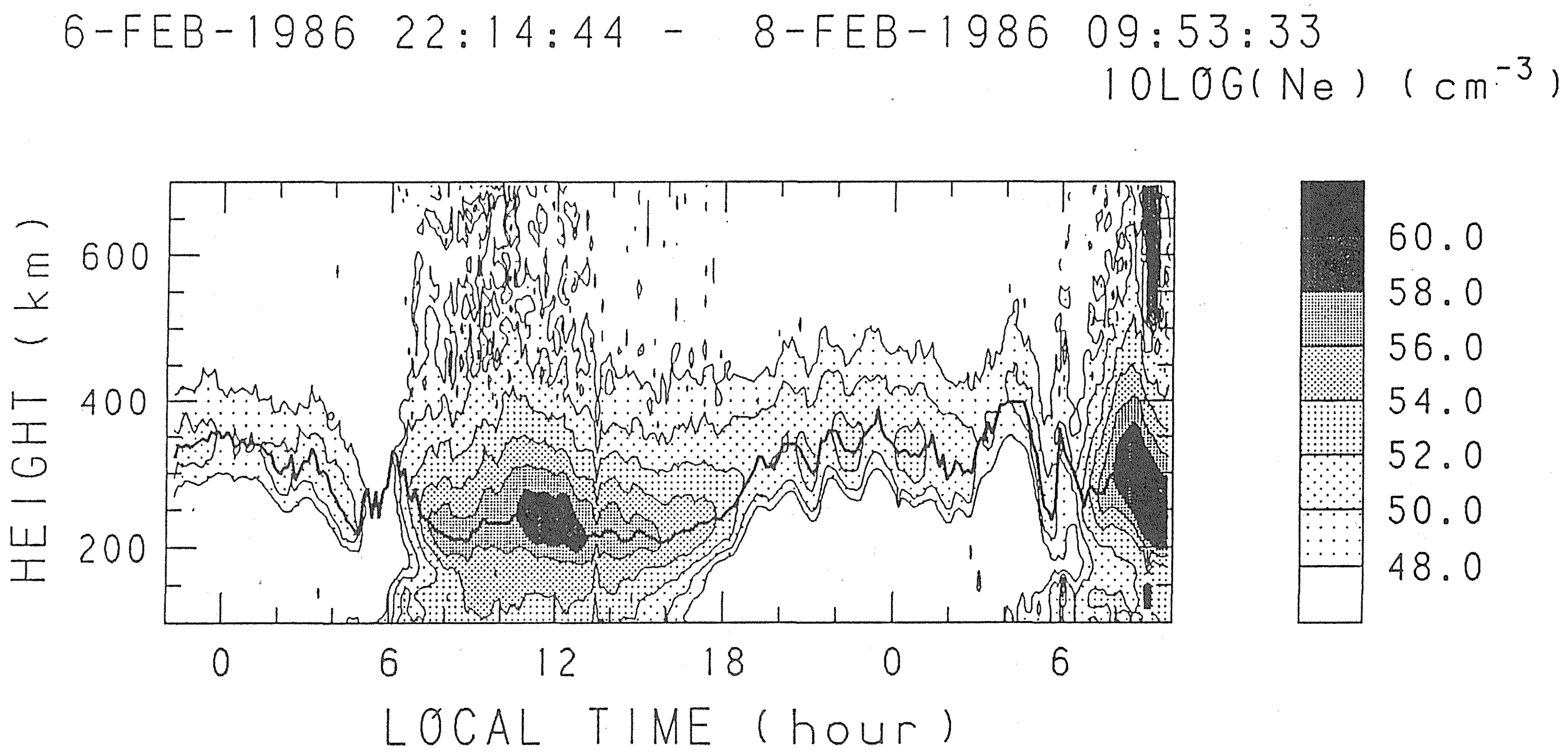

Fig. 1. Electron density measured by the MU radar during 6–8 February 1986. The heavy solid line superposed on the contour plot represents the height of the F-layer peak. The apparent predawn enhancements in E region density probably represent unrejected meteor echoes. The apparent enhancements in F region density above 500 km altitude after 9 LT on 8 February probably represent unrejected coherent echoes entering the antenna sidelobes from regions of plasma irregularities.

where C is a lumped radar system constant, R is the range to the scattering volume, and T_r is the ratio of the electron to the ion temperature (Sato et al., 1989). We normalize the measured R^2P_r profile at its peak to the F-layer peak density measured simultaneously by an on-site ionosonde to derive the MU radar "N_e" profile. This profile is accurate at the F-layer peak h_{max}, but at any other height h is in error by the ratio $[1+T_r(h_{max})]/[1+T_r(h)]$. In the worst case this could lead to a factor of two error in our N_e estimate.

3. Observations

Table 2 lists the K_p and A_p geomagnetic indices for the 6–10 February 1986 geomagnetic storm period. Geomagnetic activity commencements reported for the period of radar operation were a sudden commencement on 6 February at 1311–1313 UT (2211–2213 LT), a gradual commencement on 7 February near 09 UT (18 LT), and a sudden commencement on 7 February at 1521 UT (0021 LT on 8 February).

MU radar operation commenced at 1314 UT (2214 LT) on 6 February and terminated at 0053 UT (0953 LT) on 8 February. Thus the MU radar commenced operations almost simultaneously with the sudden commencement at 1311–1313 UT, which was followed by moderate K_p levels of 3– to 4 for the next seven 3–hour periods. The radar was in operation through the gradual commencement near 09 UT on 7 February, which saw an increase in K_p from 3+ (6–9 UT) to 6– (9–12 UT), and during the periods of large K_p values of 8– occurring later on that UT day (the following morning LT), but terminated operation prior to the occurrence of the peak K_p values of 9 reached the next morning.

Figure 1 shows the contour plot of electron density versus altitude and time as measured by the MU radar during this period. The four radar beams have been added for this display. Data were recorded every 12.5 seconds during this experiment, and we show the results averaged to 4 minutes resolution. The electron density statistical uncertainty varied during the experiment as controlled primarily by the electron density. For the F-layer peak densities of about $1.5 \times 10^{11} m^{-3}$ prevailing during most of the night of 7–8 February (the period of primary interest in this paper), the radar signal-to-noise ratio was about 0.4. With about 7000 pulses per antenna pointing direction per 4-minutes averaging period we can compute an electron density uncertainty of about 6%.

Table 2. Geomagnetic Parameters for the 6–10 February 1986 Storm

	K_p Three-Hourly Indices								A_p
Day	1	2	3	4	5	6	7	8	
6	0+	0+	1	1	[3+	3+	3–	4	11
7	3	4–	3+	6–	6–	8–	7–	8–]	82
8	7	7	7+	7–	8	8–	9	9–	202
9	9–	8–	5+	5–	5	6+	5+	4	100
10	3+	2	1	2	1	2–	3	3+	10

Brackets [ ] indicate the approximate period of MU radar operation.

Figure 2 shows the F-layer peak densities measured by the Japanese ionosonde chain arranged top to bottom in decreasing latitude (45°, 40°, 36°, 35°, 31°, 25°N). We will use these results as an aid in discussing the MU radar observations.

Several interesting features are observed in the MU radar data. First, the density structure seems normal and well-behaved throughout most of the first 24 hours of the experiment, except possibly for an anomalous rise in the layer peak height around sunrise. The effects of the early low-to-moderate geomagnetic activity appear to have had little effect on the ionosphere above the MU radar. Around 10 UT (19 LT) on 7 February, coïnciding well with the geomagnetic gradual commencement near 09 UT (18 LT) and the sharp increase in K_p from 3+ to 6−, we observe the beginning of fluctuations in F-layer density and peak height that continued most of the night and led, during following daytime, to ionospheric behavior much different than that observed the previous day. Here we see from about 19 to 03 LT perhaps five cycles in the density structure with a period of about 100 minutes. There is some irregularity in these perturbations and their period seems to increase with time, but not altitude. Phase fronts drawn through the density enhancements show clear tilts with a downward phase progression.

The results discussed thus far have been on the basis of the four combined radar beam pointing positions. We wish now to examine the differences in density behavior observed in these four beams. While the absolute density levels of these four observations were very similar, we observed important time lags between them. Figure 3 shows the correlation between the north and south beam observations for several altitudes for the time period from 1911 LT on 7 February to 0302 LT on 8 February. We will pay attention here to the altitudes of greatest signal strength, near 300 km, as the poorer statistical quality encountered at other altitudes substantially degrades their correlation results. We note that the correlation curve is well-behaved and exhibits two peaks, one at 500 seconds and the other at 108 minutes lag. The 500-second period represents the lag between the observed behaviors in the two beams, and thus concerns the phase speed at which the wave propagates in the north-south direction. The 100-minute difference between the two peaks represents the period of the large-scale periodic structure seen in Figure 1. We have performed a similar analysis with the east-west beam pair, finding correlation lag peaks at 170 seconds and 103 minutes. From these we calculate the following wave propagation characteristics: (1) a direction of travel t of $\tan(\theta) = 170/500$, or $\theta = 19°$ west of south, (2) a correlation lag T along the direction of propagation of $T^2 = (500^2 + 170^2)s^2$, or $T = 530s$, (3) a wave speed of 218.4 km/530 seconds = 410 m/s (the diagonal beams are 218.4 km apart at 300 km altitude), and (4) a horizontal wavelength of (410 m/s) × 100 minutes = 2500 km. These results are summarized in Table 3.

Table 3. Wave Propagation Parameters

Wave period	100 minutes
Direction of travel	19° west of south
Wave speed	410 m/s
Horizontal wavelength	2500 km
Vertical wavelength	290–490 km (measured) 350 km (theory)

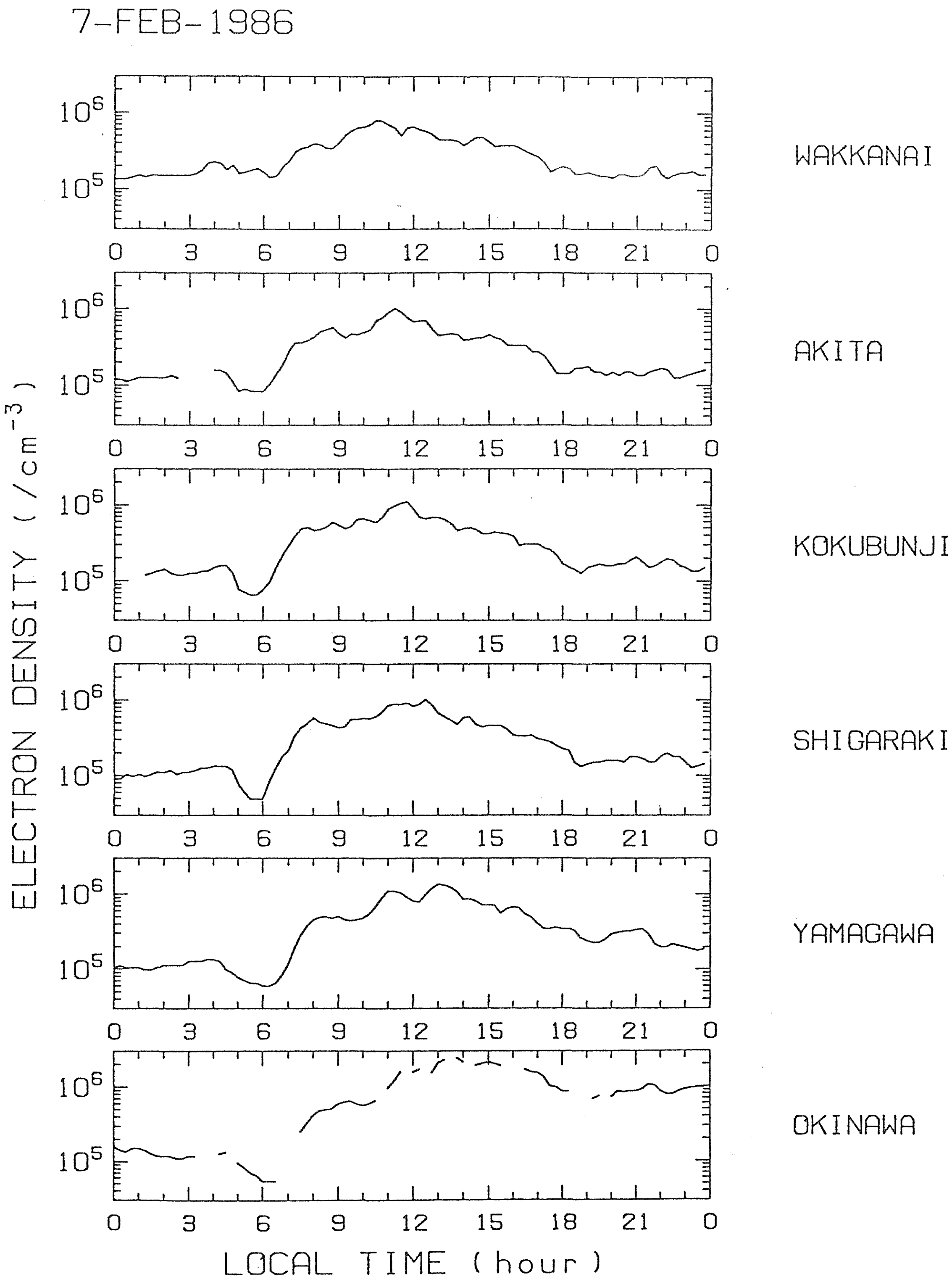

Fig. 2a. F-layer peak density results from the Japanese ionosonde chain during 7 February 1986. The latitudes of the stations are, from top to bottom, 45°, 40°, 36°, 35°, 31°, and 25°N.

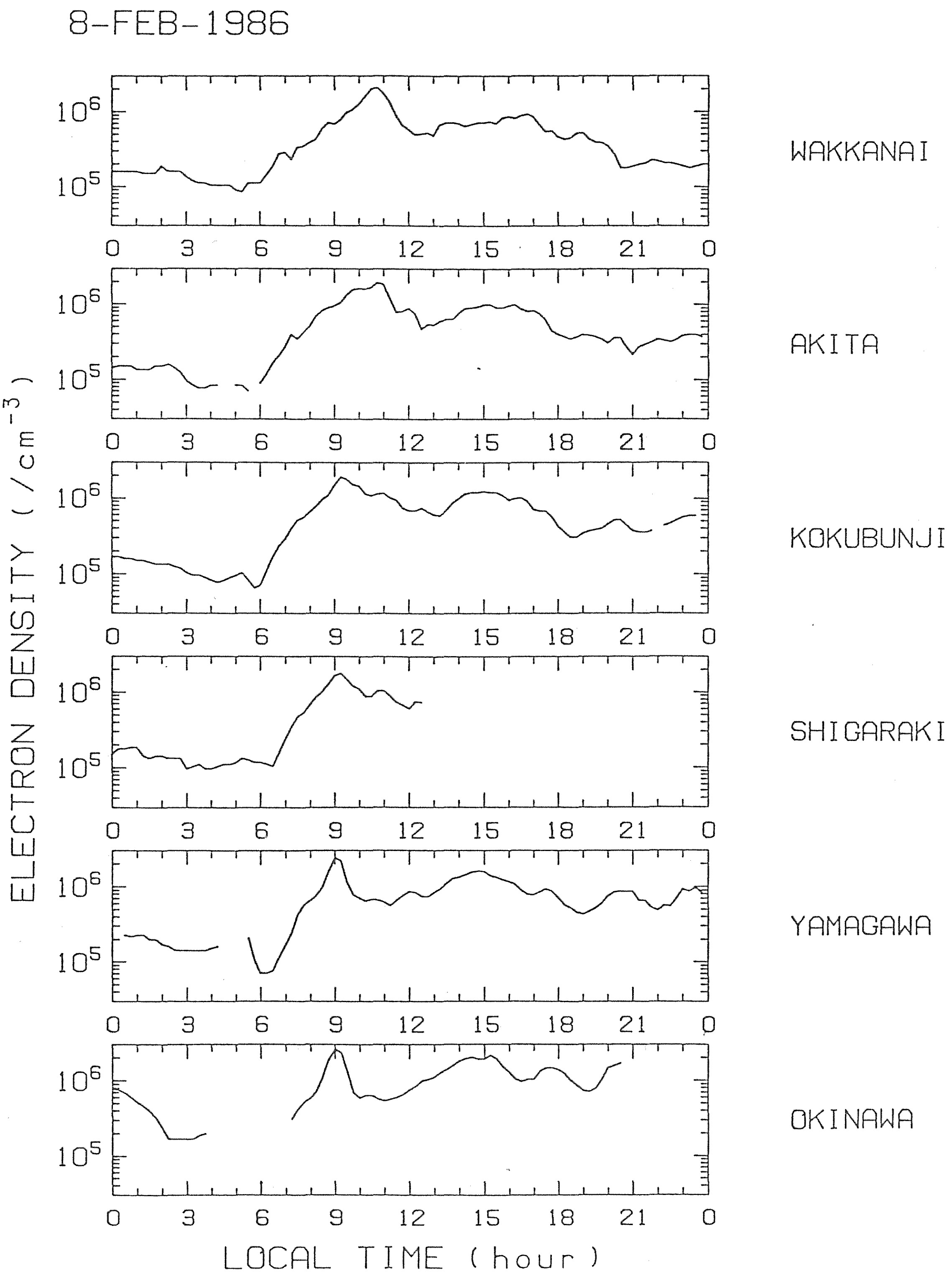

Fig. 2b. F-layer peak density results from the Japanese ionosonde chain during 8 February 1986. The latitudes of the stations are, from top to bottom, 45°, 40°, 36°, 35°, 31°, and 25°N.

The correlation magnitudes in Figure 3 are of interest. The correlation magnitude is 90% for the 500 second delay near 350 km altitude, even though the data uncertainty is 6%. Such a high correlation value for data spanning an 8-hour period indicates very stable wave propagation over the entire period. The correlation magnitude for the 100-minute delay is only about 65%, indicating that the large-scale wave cycles were not precise repetitions of each other. As pointed out previously, the wave period does appear to increase with time, and this would serve to degrade the correlation. This increase in period with time is predicted from theory (e.g., Francis, 1975; Row, 1967).

We have also cross-correlated the densities at different altitudes obtaining a vertical wavelength of 490 km. This result was critically dependent, however, upon the altitude range used. Inclusion of the poorer-quality data at higher altitudes strongly decreased the wavelength estimate (to as low as 290 km), while from physical principles (dissipation by viscosity) we would expect the phase fronts to become vertical (infinite vertical wavelength) at high altitudes (Francis, 1975). Hines (1960) gives the approximation that the ratio of the vertical and horizontal wavelengths should equal the ratio of the Brunt-Väisälä and were phase periods. Using a Brunt-Väisälä frequency of 14 minutes (appropriate to a 740 K atomic oxygen atmosphere at 320 km altitude), we then may compute a vertical wavelength of (2500 km) $\times$ (14 minutes)/(100 minutes)=350 km. This value is well in line with our estimates from the measured wave front tilts.

4. Discussion

All of the wave characteristics presented thus far match those expected from theory and observation [as summarized by Yeh and Liu (1974), Francis (1975), and others] for a classic large-scale wave launched from the auroral zone by a substorm onset - period, wavelength, speed, direction, etc. The change in F-layer peak height also is expected as a result of the wave perturbation wind forcing the layer upward or downward along the magnetic field lines. We wish now to see if the magnitude of the electron density oscillation is consistent with the existing theory of gravity-wave/ionosphere interaction. For this we use the theory developed by Hooke (1970) and reviewed by Yeh and Liu (1974), which says that the relative electron density perturbation N'/N_o is related to the perturbation wind velocity v' and wave phase velocity v_p as

$$\left(\frac{N'}{N_o}\right) = \left(\frac{v'}{v_p}\right) M$$

where M is the geometrical factor

$$M = (\mathbf{1}_k \cdot \mathbf{1}_b)\,(\mathbf{1}_{v'} \cdot \mathbf{1}_b)$$

and $\mathbf{1}_k$ is a unit vector in the direction of wave travel, $\mathbf{1}_{v'}$ is a unit vector in the direction of wind perturbation, and $\mathbf{1}_b$ is a unit vector in the direction of the magnetic field. Using our observed direction of wave propagation, and assuming that the velocity perturbation

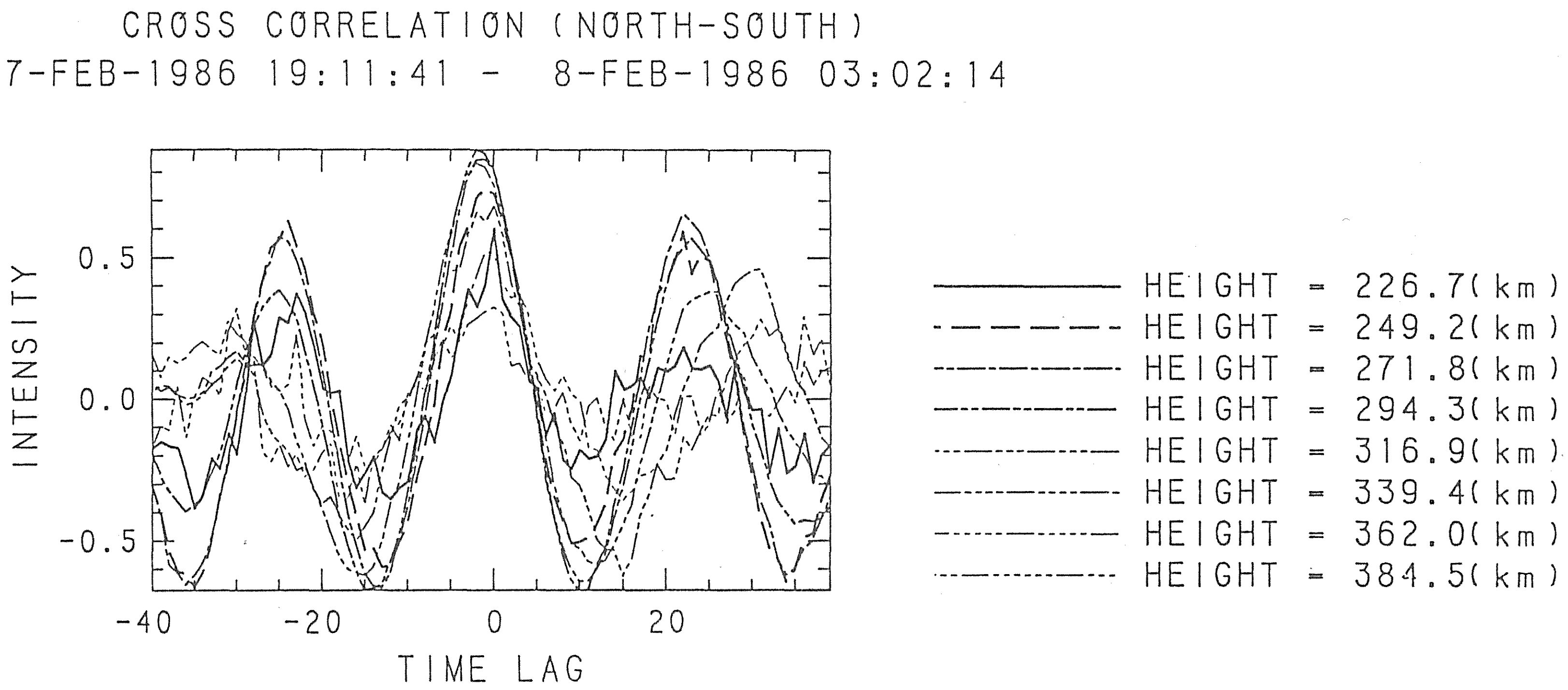

Fig. 3. Cross-correlation between the electron density observations in the north and south radar beams during the period 1911 LT on 7 February to 0302 LT on 8 February for several altitudes of measurement. Time delay is in units of 255 seconds. The highest correlation occurs near 300 km altitude, where the signal strength is strongest.

is orthogonal to this [such waves are expected to be very nearly transverse (Hines, 1960; Hooke, 1970; Francis, 1975)], we may compute the value $M = 0.46$ for our case. Now using our measured density perturbation amplitude of 20% and our measured phase velocity of 410 m/s, we find that we need a perturbation velocity of 180 m/s to account for our observed density perturbation through the action of wave dynamics. This would be a largely vertical velocity, since the wave is largely horizontally propagating and traverse. Such a vertical velocity is unheard of outside of local region of intense auroral energy input. In addition, whether this velocity were vertical or horizontal, it would have the effect of raising then lowering the F layer by some 100 km (each way)(e.g., Miller et al., 1986) whereas we observe only a modest 20 km variation in the F-layer peak. We also wish to note that the mean F layer height during this period was not unusual in comparison with measurements on other days (see the several examples in Oliver et al., 1988), so that unusually strong background winds were probably not present during the period of wave activity, and Doppler shifting effects on v_p in our N'/N_o estimates were probably not important.

We may make one additional check concerning the wave-dynamics effect. The vertical structure of the wave should produce a wind shear that would tend to cause a plasma collection effect at some altitude, similar to the sporadic-E wind-shear creation effect. We have computed the ionosphere slab thickness from our measured data and, while we do find fluctuations, we do not find a good correspondence between the periods of small thickness and of high density at the F-layer peak. Thus we do not believe that wind shear is the cause of our density increases.

Thus wave dynamics encounters great difficulties in explaining our density observations. We wish to devote the remainder of this section to a consideration of several alternative mechanisms for producing the observed density perturbation.

Energetic particle precipitation. From the continuity equation we may say that the increases in nighttime density must have come from either in-situ production of new ionization or from a net transport of ionization into the region. While there was no solar source during this nighttime period, we must consider the possibility that energetic particle precipitation was present during this strong storm, even at the low latitude of the MU radar. We have some indirect evidence from our data, however, that such ionization sources were absent. Because we are confident that we know the MU radar lumped system constant C well, we can use equation (1) to solve for the electron-to-ion temperature ratio T_r at the F-layer peak height h_{max} from radar measurements of P_r and h_{max} and ionosonde measurements of $N_e(h_{max})$. From this exercise we found that T_r remained near unity throughout the 7–8 February nighttime; this implies that sources of selective electron heating (and hence of new ionization production) were absent. Therefore, we assume that the cause of the observed density increases at night must represent a transport of ionization from other regions.

There are several specific transport effects that may be considered, including (1) wave compression, (2) lateral drift of a density gradient, (3) filling from the protonosphere, and (4) equatorial anomaly effects. These are considered separately below.

Wave compression. Francis (1975) notes that compression is not very effective at long wave periods, that the waves have predominantly transverse velocity oscillations.

Lateral drift of a density gradient. The increases in nighttime electron density could represent a lateral drift of a denser ionosphere into the MU radar region of observation. From 19 LT on 7 February to 03 LT on 8 February the fluctuations in the peak electron density over Shigaraki were on the order of 20%. Figure 2 shows the ionospheric peak densities measured by the Japanese ionosonde chain, clearly showing a higher density to the south. The peak electron density over Yamagawa averaged about 40% greater than the peak density over Shigaraki. The strength of the horizontal transport required to move the ionosphere from Yamagawa to Shigaraki (4° difference in latitude) during the 50-minute half-period of the density fluctuation is $(4^\circ \times 116\ \mathrm{km}/^\circ)/(50\ \mathrm{min} \times 60\ \mathrm{sec/min})$, or about 150 m/s. This is a very reasonable magnitude for transport by neutral winds or electric fields. Owing to the magnetic-field geometry, such a northward transport would be accompanied by a falling F-layer peak height if caused by a neutral wind but by a rising peak height if caused by an electric field. Our observation of a lowering of the F layer during periods of increasing density would then favor the neutral-wind over the electric-field mechanism. A difficulty here is that in blowing the ionosphere horizontally over 4° latitude the wind would also blow the ionosphere a similar distance (500 km) downward, owing to the magnetic dip. This is clearly impossible and would require the simultaneous action of an upward-directed electric-field force to maintain the plasma in the ionosphere. This could conceivably be an F-region dynamo electric field, produced by the wind itself [a phenomenon frequently observed by the MU radar (Oliver et al., 1988)]. But the outstanding question is: what would cause a neutral wind to oscillate north and south during the exact time interval when a gravity wave was passing from north to south, and at the same oscillation period of the wave?

Filling from the plasmasphere. Diffusion of ionization form the plasmasphere down into the ionosphere has long been recognized as a possible mechanism for the maintenance of the nighttime F-region density. From Figure 1 the background plasma density appears to be rather constant with time after sunset and throughout the several hours of wave activity. This lack of decay of the F-layer density may indicate that the layer is being maintained by a plasma flux from above. If so, the wave would have a modulating effect on the assimilation of this plasma into the ambient density. We may view here a continuous source of new ionization streaming into the top of the ionosphere balanced by a continuous loss of ionization through recombination and diffusion to determine the ambient ionosphere density profile. The deposition of the plasma flux into the ambient density is controlled largely by the F-region neutral density, or the atomic oxygen (O) density. The plasma loss via chemistry is controlled primarily by the densities of N_2 and O_2, which react with the ambient O^+ ions (to give molecular ions, which readily combine with the electrons). The plasma loss via diffusion is controlled primarily by the neutral density, or the O density. The wave will modify both the source and loss processes through their effects upon O, N_2, and O_2.

Several previous studies bear upon this modification. Yonezawa (1965) has derived an analytic approximation to show that the density produced by a flux coming into the ionosphere is proportional to the neutral number density (at the base of the ionosphere). Clark et al. (1971) have numerically simulated gravity wave behavior and the ionospheric response, finding substantial perturbations in neutral temperature and density and electron density but very different perturbation amplitudes and phases for these three parameters; in their extreme case a 10% neutral density perturbation produced a 90% electron density perturbation. Trinks and Mayr (1976) have reported satellite mass-spectrometer measurements of gravity-wave induced perturbations in the neutral composition; N_2 density amplitudes of 15%, O amplitudes of 10%, and strong phases differences between the two were seen for large-scale waves near 25° latitude. Mayr and Volland (1976) have simulated these composition perturbations, finding that the dynamic transport effects involved cause deviations from diffusive equilibrium to prevail throughout the upper atmosphere, leading to different perturbation amplitudes and phases for the different atmospheric gases and for the temperature, largely consistent with the satellite observations. All of these analyses and simulations pertain to the type of large-scale waves seen by the MU radar. They indicate that a small neutral density perturbation can produce a larger ionospheric density perturbation. They indicate that substantial perturbation amplitudes in N_2 and O can exist. They indicate that the N_2 and O density perturbations can have different phases; this means that the ionization source and loss perturbations will be out of phase, and the resulting ambient plasma density will be modulated accordingly.

Both qualitatively and quantitatively, then, we find no inconsistency between our observed wave-modulated electron densities and the concept of gravity-wave modulation of the assimilation of a plasmashperic flux into the ambient density. We have the possible picture, not of a nighttime decaying F layer, but of one maintained in equilibrium by an incoming plasma flux, analagous to the maintenance of the daytime F layer by an incoming photon flux. In either system, modulation of the background atmosphere, by a gravity wave or any other means, will modulate the ionosphere equilibrium density. The nighttime maintenance of the F layer above Shigaraki does not seem to be an unusual or storm-related phenomenon, for the examples presented by Oliver et al. (1988) indicate that the ionosphere there regularly decays after sunset to an early nighttime level below which it does not decay for the remainder of the night.

Equatorial anomaly effects. Figure 2 shows that the F-layer peak density increased toward the equator during the period of the wave activity. Equatorial anomaly activity is a possible explanation for this low-latitude maximum, and we can then ask if the nighttime density increases at Shigaraki correspond to the outer fringe of the equatorial "fountain" effect. The equatorial anomaly is produced by equatorial electric fields which force the plasma to high altitudes, from which it diffuses down magnetic field lines to higher latitudes. The Shigaraki field line reaches the magnetic equator at an altitude exceeding 2000 km. Simulations (e.g., Hanson and Moffett, 1966) indicate that substantial ionization is not lifted this high, but they also show that the off-equator electric fields play an important role in driving the diffusing plasma directly to higher magnetic latitudes, beyond the field lines to which substantial plasma is lifted at the equator. Shigaraki rests on the fringe of the equatorial anomaly in these simulations, and during the February 1986 period of great electrical agitation it is conceivable that such effects could have extended to Shigaraki. As a cause for the periodic nighttime increases in density observed during the wave period, however, we would have to invoke a periodic excitation in the electric fields at the equator. We have examined magnetograms from the Asian sector, from Memambetsu, Kanoya, Kakioka, and Guam (dip latitudes 38°, 30°, 26°, and 6°, respectively) for this periodicity without success.

Of the arguments considered above to explain the periodic increases in F-layer density during the wave passage, the one invoking an incoming flux of plasma, modulated by the wave's effects upon the background atmosphere, appears to have the fewest objections. In this scenario all observed effects are caused by the wave and act upon the existing ionosphere without any need to invoke unusual processes or fortuitous coincidence of events.

After the periodic wave-like motion seen in the 19–03 LT time period of 7–8 February, we observed some even larger excursions in F-layer peak height until about 07 LT on 8 February. This was followed during the ensuing morning daylight period by the development of very large peak electron densities and a low and decreasing peak height until observations terminated at 0953 LT. For comparison, the peak densities measured by the Japanese ionosonde chain during this period are shown in Figure 2. Here we see correlated density perturbations at all latitudes but a particularly evident and isolated density increase to the south near 9 LT. The simultaneous density increase and layer peak-height decrease observed at Shigaraki forms an interesting geophysical problem. Normally, when a neutral wind or electric field forces the F layer downward in the daytime ionosphere, the peak density decreases owing to the increased rate of chemical loss. While we could examine several possible explanations for this effect, as we did for the wave period, we have even fewer constraints in our arguments here. Let it suffice to say that we see fewer objections, once again, to an explanation in terms of an in-flux of plasma form the top of the ionosphere.

5. Note on the Use of the MU Radar for Wave Detection

The MU radar was in operation during the 6–8 February 1986 storm period by chance. Though not designed to observe wave propagation, the four-beam experiment employed was successful in doing so. The ability to observe in different directions simultaneously is a major unique and novel feature of the MU radar which gives it capabilities for wave observation not previously available in ionospheric radars. In his review of gravity waves Francis (1975) noted that the determination of horizontal wave speeds and directions of motion was (at that time) impossible with single-station measurements. He also noted that an array of stations (with assumed fixed spatial distribution) would be sensitive to only a limited range of horizontal wavelengths, for if the station spacing were too small compared to the horizontal wavelength the wave would be essentially in phase across the array, while if the spacing were too large the waveform would change as it propagated between array elements. The MU radar alleviates these objections to some degree. First, it is a single station, but because of its flexible phased-array design it can observe different horizontal locations as if it were an array of sensors. Second, its flexible pointing capability makes it possible to adjust the dimensions of the horizontal observing grid and to use a flexible number of grid points such that waves over a broad range of horizontal dimensions can be detected. Certainly the results shown in this paper evidence the ability of the MU radar to detect the very long horizontal wavelengths with a standard four-beam experiment providing observation points on the order of only 200 km apart. Hearn and Yeh (1977) have detected medium-scale gravity waves with the Arecibo incoherent scatter radar (pointed vertically), having deduced horizontal wavelengths as small as 140 km. Yeh et al. (1979) have discussed the benefit of having a direct measurement of the horizontal structure. The MU radar could easily observe the horizontal structure of such waves by inserting additional beam positions to provide adequate spacing to sample them. The limitation in the number of beams used comes in the practical statistical considerations, for the variance in the estimates of the observed ionospheric parameters (e.g., electron density) at any one position increases linearly with the number of positions used. A 16-beam experiment can cover a much larger range of horizontal scales than a 4-beam experiment but will incur twice the uncertainty (standard deviation). Thus an important compromise arises between time resolution and grid coverage.

6. Summary

The MU radar conducted an incoherent scatter power profile experiment during the large geomagnetic storm of 6–8 February 1986. Nearly simultaneously with the increase in the K_p index from 3+ to 6− we observed the beginning of eight hours of wave activity in the F-region density showing a 100-minute period during the nighttime period of 7–8 February. The radar experiment used four observing positions. Correlation of the behaviors in these beams allowed the identification of the wave phase speed (410 m/s), direction of travel (19° west of south), horizontal wavelength (2500 km), and vertical wavelength (290–490 km). This wave had the propagation characteristics of a classic large-scale gravity wave launched by an auroral substorm. We judged, however, that the neutral wind perturbation needed to create the observed density perturbation through wave dynamics was excessive and inconsistent with the observation of only modest changes in the F-layer peak height. Of several alternate possibilities considered to explain the density increases, one invoking a flow of plasma into the top of the ionosphere, and a wave-induced modulation of the assimilation of this flux into the ambient density, seemed to encounter the fewest difficulties. The following daytime period saw the development of very high electron densities during a period when the F-layer peak height was decreasing. Again we speculated that this density increase was due to an in-flux of plasma from above.

7. Acknowledgements

The authors wish to thank Arthur Richmond, Anthony Van Eyken, and Maura Hagan for useful discussion concerning the data and interpretation. The authors are indebted to the staff of the Radio Atmospheric Science Center and the Department of Electrical Engineering of Kyoto University for their helpful support. One of us (WLO)was supported for this work as a Visiting Research Scholar at Kyoto University and as a Visiting Associate Professor at the Radio Atmospheric Science Center. The MU radar belongs to and is operated by the Radio Atmospheric Science Center of Kyoto University.

8. References

Clark, R.M., K.C. Yeh, and C.H. Liu, Interaction of internal gravity waves with the ionospheric F2-layer, *J. Atmos. Terr. Phys.*, 33, 1567–1576, 1971.

Francis, S.H., Global propagation of atmospheric gravity waves: A review, *J. Atmos. Terr. Phys.*, 37, 1011–1058, 1975.

Fukao, S., T. Sato, T. Tsuda, S. Kato, K. Wakasugi, and T. Makihara, The MU radar with an active phased array system, 1. Antenna and power amplifiers, *Radio Sci.*, 20, 1155–1168, 1985.

Fukao, S., T. Tsuda, T. Sato, S. Kato, K. Wakasugi, and T. Makihara, The MU radar with an active phased array system, 2. In-house equipment, *Radio Sci.*, 20, 1169–1176, 1985.

Hanson, W.B., and R.J. Moffett, Ionization transport effects in the equatorial F region, *J. Geophys. Res.*, 71, 5559–5572, 1966.

Hearn, A.L., and K.C. Yeh, Medium scale TID's and their associated internal gravity waves as seen through height-dependent electron density power spectra, *J. Geophys. Res.*, 82, 4983–4990, 1977.

Hines, C.O., Internal gravity waves at ionospheric heights, *Can. J. Phys.*, 38, 1441–1481, 1960.

Hooke, W.H., The ionospheric response to internal gravity waves, 1. The F_2 region, *J. Geophys. Res.*, 75, 5535–5544, 1970.

Kato, S., T. Ogawa, T. Tsuda, T. Sato, I. Kimura, and S. Fukao, The middle and upper atmosphere radar: First results using a partial system, *Radio Sci.*, 19, 1475–1484, 1984.

Kato, S., T. Tsuda, M. Yamamoto, T. Sato, and S. Fukao, First results obtained with a middle and upper atmosphere (MU) radar, *J. Atmos. Terr. Phys.*, 48, 1259–1267, 1986.

Mayr, H.G., and H. Volland, Composition waves in the thermosphere, *J. Geophys. Res.*, 81, 671–676, 1976.

Miller, K.L., D.G. Torr, and P.G. Richards, Meridional winds in the thermosphere derived from measurement of F_2 layer height, *J. Geophys. Res.*, 91, 4531–4535, 1986.

Oliver, W.L., S. Fukao, T. Sato, T. Tsuda, S. Kato, I. Kimura, A. Ito, T. Saryou, and T. Araki, Ionospheric incoherent scatter measurements with the MU radar: Observations of F-region electrodynamics, *J. Geomag. Geoelec.*, 40, 963–965, 1988.

Row, R.V., Acoustic gravity waves in the upper atmosphere due to a nuclear detonation and an earthquake, *J. Geophys. Res.*, 72, 1599–1610, 1967.

Sato, T., A. Ito, W. Oliver, S. Fukao, T. Tsuda, and S. Kato, Ionospheric incoherent scatter measurements with the MU radar: Techniques and capability, *Radio Sci.*, 24, 85–98, 1989.

Trinks, H., and H.G. Mayr, Large-scale neutral composition gravity waves in the thermosphere observed by ESRO 4, *J. Geophys. Res.*, 81, 4023–4026, 1976.

Vickrey, J.F., W.E. Swartz, and D.T. Farley, Ion transport in the topside at Arecibo, *J. Geophys. Res.*, 84, 7307–7314, 1979.

Yeh, K.C., and C.H. Liu, Acoustic-gravity waves in the upper atmosphere, *Rev. Geophys. Space Phys.*, 12, 193–216, 1974.

Yeh, K.C., C.H. Liu, and A.L. Hearn, Propagation of gravity wave spectra in the thermosphere, *J. Geophys. Res.*, 84, 834–838, 1979.

Yonezawa, T., Maintenance of ionization in the nighttime F_2 region, *Space Res.*, V, 49–60, 1965.